Acta Cryst. (1980). A**36**, 390–398

An Investigation of the Electron Density in Li_3N Using Compton Scattering

BY P. PATTISON AND J. R. SCHNEIDER

*Hahn-Meitner-Institut für Kernforschung, D-*1000 *Berlin* 39, *Glienicker Strasse* 100, *Federal Republic of Germany*

(*Received* 10 *September* 1979; *accepted* 10 *December* 1979)

Abstract

Compton profiles of Li_3N have been measured along three crystallographic orientations. The profiles are compared with theoretical curves for neutral atoms (Li^0 and N^0) and for an ionic model (Li^+ and N^{3-}). The wave functions for the N^{3-} ion have been taken from a recent Watson-sphere model in which an additional spherical potential is introduced in order to simulate the stabilizing influence of the crystal environment. The shape of the theoretical N^{3-} profile could be adjusted to achieve good agreement between experimental results and the ionic model for a Watson radius of $r_W = 1{\cdot}2$ Å. This is in some disagreement with the results of a recent X-ray diffraction study on Li_3N [Schulz & Schwarz (1978). *Acta Cryst.* A**34**, 999–1005] who favoured a value of $r_W = 1{\cdot}38$ Å. Possible reasons for the discrepancy, both experimental uncertainties as well as more fundamental differences between charge and momentum density quantities, are discussed. In addition, a significant anisotropy in the experimental Compton profiles was observed, particularly between measurements made with the scattering vector within and perpendicular to the Li_2N layers, which is inconsistent with a pure ionic picture of the chemical bonding in Li_3N. Using the Fourier transform of the experimental Compton profile as an aid for the interpretation of this anisotropy it is concluded that there is a distortion of the N^{3-} ions due both to the anisotropic coordination of the neighbouring Li^+ ions and to the overlap with other nitrogen ions within the Li_2N layers. Solid-state calculations are needed in order to gain a better understanding of the chemical bonding in Li_3N and experimental Compton profiles should provide a powerful tool to test these calculations.

1. Introduction

The ionic conductor Li_3N has recently been the subject of a considerable amount of research activity. This interest has stemmed partly from its unusual properties as a lithium conductor with a high and extremely anisotropic conductivity even at room temperature, suggesting possible applications as a solid electrolyte. On the other hand, because of its highly symmetric structure with only four atoms per elementary cell, Li_3N is accessible to theoretical treatment and is regarded as a useful model of an ionic crystal with a highly polarizable N^{3-} ion. In addition, the basic mechanism of the bonding in Li_3N itself has been in dispute for some time. An extensive summary of the many types of investigations made of this material is contained in a review article by Rabenau (1978).

Lithium nitride crystallizes in space group *P6/mmm*, and its structure can be described as alternating layers of Li_2N divided by layers of pure Li. The N atoms occupy the centre of the elementary cell within a hexagonal array of Li atoms, as illustrated in Fig. 1. Two additional Li atoms, which sit above and below each N, form the Li layers. In the Li layers the atoms are labelled Li(1) and in the Li_2N layers the Li atoms are labelled Li(2). At room temperature the interatomic distances Li(1)–N and Li(2)–N are 1·938 and 2·107 Å, respectively. Neighbouring N atoms are separated by 3·649 Å within the layers and 3·877 Å between layers.

It is tempting to suggest that the bonding could be purely ionic due to the formation of the closed-shell ions Li^+ and N^{3-}. However, this electronic configuration would lead to colourless crystals, whereas the crystals are actually ruby red. Nevertheless, strong support for the ionic picture can be found in the results

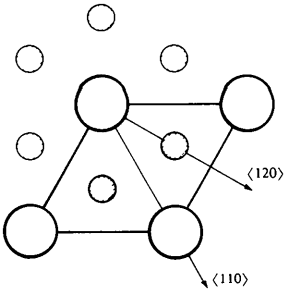

Fig. 1. A cut through the Li_3N crystal structure showing part of a Li_2N layer. Large spheres indicate the nitrogen sites. Atoms which form the pure lithium layers are situated directly above and below each nitrogen.

0567-7394/80/030390-09$01.00

of a recent X-ray diffraction measurement performed by Schulz & Schwarz (1978). In addition, polarized infrared and Raman spectra were measured on Li_3N by Chandraseka, Bhattacharya, Migoni & Bilz (1978). A rigid-shell model with eight parameters, including the anisotropic polarizability of nitrogen ions, yielded an excellent fit to the observed phonon frequencies and again the authors conclude that Li_3N is the first known compound in which nitrogen ions are close to an anomalous N^{3-} state.

The stimulus for the present Compton-scattering study was provided by the X-ray diffraction work by Schulz & Schwarz (1978) who compared their experimental results with theoretical structure factors derived from a Watson-sphere model for N^{3-} (Schwarz & Schulz, 1978) and a free-ion Li^+. Very satisfactory agreement between theory and experiment was found after adjusting the Watson radius to $r_W = 1{\cdot}38$ Å. We consider lithium nitride to be a useful model substance also for a Compton study since it has the advantage of a relatively simple crystal structure. This is an important point because the Compton profile is a single-centred quantity, which implies that there will be a superposition of information from all parts of the unit cell. Although this is an advantage when the structure has a high symmetry, the effect of this superposition undoubtedly complicates the interpretation of data from more complex crystals. The presence of the diffuse nitrogen ion leads to an electronic behaviour which is not yet fully understood. A Watson-sphere model, which introduces an additional stabilizing spherical potential, can provide only a starting point for a description of the solid state.

A measurement of the electron momentum density can first be used to assess the accuracy of the ionic model of the bonding in Li_3N. To do this we will compare the experimental Compton profile with the Watson-sphere model using the same wave functions as were calculated by Schwarz & Schulz (1978) and used by them to evalute their X-ray diffraction data. In addition, any anisotropy which is found in the momentum distribution (which necessarily lies outside the scope of the isotropic Watson model) will provide experimental criteria against which to test any improved models of the electronic structure of this material. In the absence of any solid-state model specifically for Li_3N, we will also make use of the Fourier transform of the Compton profiles to interpret our experimental results. Since this transformation places the results on a position rather than a momentum scale, we can draw on our knowledge of the structure of the crystal as well as our better intuitive grasp of bonding concepts in position space.

In the following section the technique of Compton scattering is briefly summarized. The method of obtaining the Compton profile from the wave functions supplied by Schwarz (1979) is presented in § 3, together with some numerical results for the N^{3-} ion. In § 4 the practical details of the present experiment are described and the experimental results are tabulated. Following a discussion of these results in § 5, some concluding remarks and suggestions are given in the final section.

2. Compton scattering

In a Compton-scattering experiment, the energy distribution of photons which have been inelastically scattered through a fixed angle by a body of electrons can be related to the initial electron momentum distribution in the target. Within the impulse approximation, the scattering cross section is proportional to the Compton profile, $J_K(p_z)$, which is the projection of the target electron momentum distribution $\rho(\mathbf{p})$, onto the experimental scattering vector, $\mathbf{K}$. The Compton profile can be expressed in terms of the electron momentum wave function, $\chi(\mathbf{p})$, by

$$J_K(p_z) = \sum_i \int\int_{p_x p_y} |\chi_i(\mathbf{p})|^2 \, dp_x \, dp_y, \qquad (1)$$

where p_z is chosen parallel to $\mathbf{K}$, and the summation i runs over each electron in the atom, molecule or unit cell. Hence the Compton profile is not a measure of the momentum density itself, but rather an integration of $\rho(\mathbf{p})$ over planes perpendicular to the scattering vector. A description of the technique of Compton scattering and an assessment of the validity of the various assumptions leading to the definition of the Compton profile is given in the collection of review papers edited by Williams (1977).

The Fourier transform of a Compton profile can provide an additional insight into the formation of bonds in a crystal. Starting from the Fourier transform of the momentum density, we can write

$$B(\mathbf{t}) = \sum_i \int |\chi_i(\mathbf{p})|^2 \exp(-i\mathbf{p}.\mathbf{t}) \, d\mathbf{p}$$

$$= \sum_i \int \psi_i(\mathbf{r}) \, \psi_i^*(\mathbf{r} + \mathbf{t}) \, d\mathbf{r}, \qquad (2)$$

where $\psi_i(\mathbf{r})$ is the position-space electron wave function. For a crystal, (2) can be rewritten in terms of the Bloch functions $\varphi_{\nu,\mathbf{k}}(\mathbf{r})$, where the summation must now run over all values of the crystal momentum $\mathbf{k}$ for each band ν. For completely filled energy bands, the summation over $\mathbf{k}$ can be avoided by replacing the Bloch functions, $\varphi_{\nu,\mathbf{k}}(\mathbf{r})$, by the $\mathbf{k}$-independent Wannier functions, $a_\nu(\mathbf{r})$. It is then possible to recover the simple form of (2). In the case of a directional Compton-profile measurement, the momentum density has been projected onto p_z, and hence the Fourier transform yields only $B(z)$, where z is parallel to p_z. Therefore, the

experimental Compton profile of an insulator can be Fourier transformed to provide the autocorrelation function of the crystal Wannier functions along the direction defined by the scattering vector. It is hoped that this relation between the electronic wave functions and Compton-scattering data can facilitate the interpretation of experimental results even in the absence of a theoretical model. In particular, an important condition on the zeros in $B(t)$ follows directly from (2). Since the Wannier functions for all electrons on each transitional lattice site must be mutually orthogonal, it is possible to write immediately $B(\mathbf{R}_j) = 0$ for all transitional lattice vectors $\mathbf{R}_j$ (Schülke, 1977). In addition to the orthogonalization condition which leads to zeros at all $\mathbf{R}_j$, the autocorrelation function at the origin, $B(0)$, simply expresses the normalization of the wave functions, *i.e.* for Li_3N one obtains $B(0) = 16{\cdot}0$.

3. Form factors and Compton profiles for N^{3-}

Schwarz & Schulz (1978) have described a calculation of the wave functions for a N^{3-} ion using a model suggested by Watson (1958). This consists of simulating the ionic environment in a crystal by embedding the ion under consideration in a hollow sphere which carries a uniformly distributed charge Q. The value of Q was assumed to be +3, corresponding to the negative charge of the ion itself, and the radius r_W of the Watson sphere provides a variable parameter. This external Watson potential is added to the ion potential, and self-consistent solutions can then be obtained for negative ions which would otherwise be unstable. A change in the value of r_W modifies mainly the spatial extent of the wave functions, whereby the choice of a small r_W, for example, leads to a more contracted wave function. Therefore, this one-parameter, isotropic model can be expected to provide only a rough guide to the shape of the wave functions in the crystal.

The wave function $\psi_{nlm}(\mathbf{r})$ for an electron in an orbital with quantum numbers n, l and m can be written as a product of a radial term, $R_{nl}(r)$, and an angular term, $Y_{lm}(\mathbf{r}/r)$. The charge density, $\rho_{nlm}(\mathbf{r})$, is then obtained by taking the square of the modulus of $\psi_{nlm}(\mathbf{r})$ and the form factor, $f_{nlm}(\mathbf{s})$, is the Fourier transform of the charge density. In order to obtain the form factor for an atom or ion, it is necessary to take a spherical average. It is immaterial whether one calculates $f_{nlm}(\mathbf{s})$ and averages over all orientations of $\mathbf{s}$, or first averages $\rho_{nlm}(\mathbf{r})$ before calculating $f_{nlm}(\mathbf{s})$ (see, for example, Bonham & Fink, 1974). Therefore, by taking the spherical average of the charge density, one need only consider the radial term, $R_{nl}^2(r)$. By expanding the exponential in Bessel functions, the Fourier transform of the charge density can be written

$$f_{nl}(s) = \int_0^\infty R_{nl}^2(r) j_0(sr) r^2 \, dr. \qquad (3)$$

Only the zero-order Bessel function, $j_0(sr)$, is required since the charge density has been spherically averaged. The total form factor for the atom, $F(s)$, is the sum of the weighted orbital contributions, where the weighting factor is the number of electrons in each shell. Form factors for N^{3-} and O^{2-} obtained in this way using the wave functions from the Watson-sphere calculation have been published by Schwarz & Schulz (1978). An inspection of the form-factor curve for N^{3-} reveals that a change of 0·2 Å in the Watson radius modifies $F(s)$ by about 5% in the region of the lowest-order reflexions in Li_3N ($0{\cdot}1 < \sin\theta/\lambda < 0{\cdot}3$).

In order to calculate the Compton profile, one must first Fourier transform the position-space wave function, $\psi_{nlm}(\mathbf{r})$, to momentum space,

$$\chi_{nlm}(\mathbf{p}) = \int R_{nlm}(r) j_l(pr) r^2 \, dr Y_{lm}(\mathbf{p}/p). \qquad (4)$$

The momentum density, $\rho_{nlm}(\mathbf{p})$, obtained by squaring the momentum-space wave function, can then be spherically averaged to yield

$$\rho_{nl}(p) = |\int R_{nl}(r) j_l(pr) r^2 \, dr|^2. \qquad (5)$$

The Compton profile for a spherical-symmetric momentum density is given by

$$J_{nl}(q) = \tfrac{1}{2} \int_q^\infty \rho_{nl}(p) p \, dp. \qquad (6)$$

The total Compton profile for the atom, $J(q)$, is then obtained by summing the orbital contributions, $J_{nl}(q)$, weighted by the orbital occupancy. The Compton profiles derived from the numerical wave functions supplied by Schwarz (1979) are presented in Table 1

Table 1. *Compton profiles for* N^{3-} *calculated from the Watson-sphere model using the wave functions supplied by Schwarz* (1979)

	Watson radius r_w (Å)		
p (a.u.)	1·0	1·2	1·4
0·00	4·5686	4·9022	5·2042
0·10	4·5371	4·8655	5·1633
0·20	4·4352	4·7420	5·0169
0·30	4·2492	4·5080	4·7271
0·40	3·9750	4·1593	4·2929
0·50	3·6263	3·7220	3·7607
0·60	3·2308	3·2407	3·1969
0·70	2·8207	2·7604	2·6588
0·80	2·4236	2·3147	2·1819
0·90	2·0588	1·9225	1·7807
1·00	1·7366	1·5906	1·4549
1·20	1·2289	1·0968	0·9944
1·40	0·8817	0·7815	0·7155
1·60	0·6527	0·5839	0·5457
1·80	0·5028	0·4586	0·4382
2·00	0·4031	0·3761	0·3661
3·00	0·1969	0·1954	0·1949
4·00	0·1188	0·1183	0·1179
5·00	0·0732	0·0738	0·0730

for various values of the Watson radius, r_W. It can be seen that a change in r_W of 0·2 Å modifies the peak height of the N^{3-} Compton profile by about 5%.

It is useful to compare (3) and (5), which define the spherically averaged form factor and momentum density respectively. The fundamental difference between the two functions concerns the order in which the operations of squaring and Fourier transforming are performed. However, it is interesting to note from (5) that, even when calculating the spherically averaged orbital momentum density, one must take into account the original symmetry of the orbital (*i.e.* the appropriate order spherical Bessel function must be used). The form factor, on the other hand, is obtained from the spherically averaged charge density and hence only the zero-order Bessel function is required. This will lead to a different weighting of a $2p$ orbital, for example, when calculating the two functions. In particular, because of the shape of the zero- and first-order Bessel functions, the $2p$ terms in the momentum density will be more sensitive to the outer part of the radial wave function, whereas the spherically averaged form factor will depend more strongly upon the region close to the origin. This serves to emphasize the complementary nature of the form factor and the Compton profile, and implies that an approximate wave function may provide a satisfactory description of only one of these electron-density properties.

The autocorrelation function $B(t)$ can be derived from the Compton profile by making a one-dimensional Fourier transform of the total profile,

$$B(t) = \int J(q) \exp(-iqt)\, dq, \qquad (7)$$

or, alternatively, each orbital can be transformed separately and summed. In Fig. 2 we show $B_{nl}(t)$ for each orbital derived from the N^{3-} Watson-sphere model (with a Watson radius of 1·2 Å). Beyond about 1 Å there are significant contributions only from the $n = 2$ orbitals, and this method of analysis therefore provides a convenient method of separating orbitals. Note that the long-range part of $B_{2p}(t > 2{\cdot}4$ Å) is always negative, and beyond about 3 Å this contribution will dominate the total $B(t)$ for $N^{3-}(1s^2\ 2s^2\ 2p^6)$. The negative part of $B_{nl}(t)$ arises from correlation between positive and negative regions of the position-space wave function, and the angular part of the wave function therefore plays a crucial role in determining the sign of $B(t)$. The functional form of $B(t)$ for atoms and molecules, as well as its relation to other electron-density quantities, has been discussed by Weyrich, Pattison & Williams (1979).

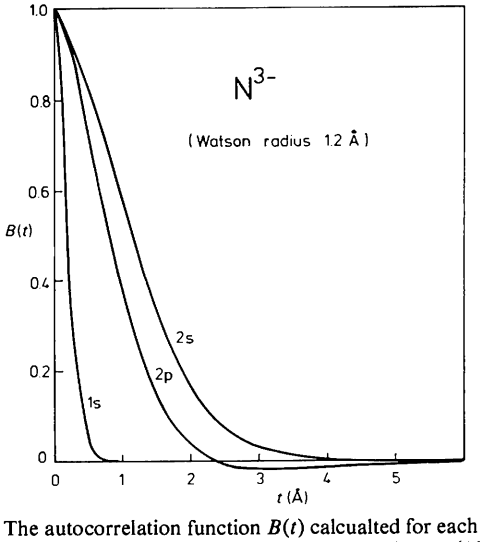

Fig. 2. The autocorrelation function $B(t)$ calcualted for each orbital from the N^{3-} wave functions provided by Schwarz (1979).

4. Experimental method and results

The most versatile system available at present for Compton-scattering studies consists of a high-energy gamma-ray source and a solid-state detector to analyse the energy spectrum of the scattered radiation. An apparatus of this type has been constructed at the Hahn-Meitner-Institut in Berlin, and its operation and performance has been described in detail elsewhere (Pattison & Schneider, 1978; Schneider, Pattison & Graf, 1979). The stability of the equipment together with the high incident photon flux allows data of good statistical accuracy to be collected in a matter of days. There is, however, the drawback of rather limited momentum resolution, which presents some difficulties when investigating the momentum distribution in metals. Hence, there is a preference towards the study of materials in which covalent or ionic bonding is present, in order to avoid the sharp breaks in the momentum density associated with Fermi surface structure. A material such as lithium nitride should therefore be very suitable for Compton-scattering work.

In the present experiment, gamma-rays from a 200 Ci ($7{\cdot}4 \times 10^{12}$ Bq) ^{198}Au source are scattered by the sample through an angle of 165°. The incident photon energy is 412 keV, and the energy distribution of the scattered photons peaks at 160 keV. A series of collimators define the incident and scattered beam paths, producing a Gaussian angular divergence with a FWHM of 1·2°. The combined effects of detector resolution and beam divergence produce a total momentum resolution of 0·41 a.u. FWHM. An extensive review of the experimental technique has been given by Weiss, Reed & Pattison (1977), while the data-analysis procedure has already been described in detail (Cooper, Pattison & Schneider, 1976).

Profiles were measured along three crystallographic directions, using the same sample in each case. The

sample was cylindrical in shape (radius 3·8, length 4·3 mm) oriented with ⟨001⟩ lying along the axis of the cylinder. The quality of the crystal, as well as its orientation, was checked by measuring rocking curves for several reflections in different volume elements using a gamma-ray diffractometer [for a description of the diffractometer see Schneider (1974) and Schneider, Pattison & Graf (1979)]. The crystal was found to be of very good quality, with a mosaic spread of only about 3′ over large regions of the sample volume.

Compton measurements were performed with the scattering vector perpendicular to the planes (001), (100) and (110), which correspond to the directions ⟨001⟩, ⟨120⟩ and ⟨110⟩. Following the normal convention, the Compton profiles will always be labelled according to their (h, k, l) index. The $B(z)$, on the other hand, will be identified by their direction $\langle u,v,w\rangle$ in position space, *i.e.* in the direct lattice. The two orientations of the scattering vector in the Li_2N plane are indicated in Fig. 1. The crystals were aligned in the Compton-scattering chamber to within ±2°. Each measurement took about 4 d, and 10^7 counts were collected in the (001) profile and 5×10^6 counts in the other two profiles. With a channel spacing of 0·03 a.u. of momentum, the corresponding peak counts were 10^5 for (001) and 5×10^4 for (100) and (110) profiles.

Particular care must be taken concerning the effect of resolution on the Compton profile. Rather than attempting to deconvolute the data, the processing is designed only to remove the effects of asymmetry in the experimental resolution function. Therefore, it is still necessary to convolute any theoretical profile with a Gaussian of 0·41 a.u. FWHM before comparing theory and experiment. It should be noted that the effect of experimental resolution on $B(z)$, the Fourier transform of the Compton profile, is to multiply the true curve with a Gaussian function. This progressively dampens the long-range information in $B(z)$, and thus sets a limit of about 7 or 8 Å on the range of the autocorrelation which can be observed. More precisely, the present resolution reduces the amplitude of $B(z)$ by a factor of two at 3·56 Å and by a factor of ten at 6·49 Å.

Multiple scattering can be a serious source of systematic error in Compton-profile measurements. For this reason, Monte Carlo programs have been developed which have been used successfully to calculate the contribution from those photons which have scattered more than once in the sample. Such a program has been used in the present case (see Felsteiner & Pattison, 1976) where the total amount of multiple scattering was in any case low (<3%). An additional problem in the present experimental system concerns the difficulty of ensuring the purity of the incident 412 keV photons. Because it is unavoidable that some of these photons scatter in the source itself before reaching the sample, there is a small, low-energy tail on the spectral distribution of the incoming photons. This leads in turn to a slight asymmetry in the profile (~2%) and therefore only the high-energy side of the experimental profile is used for quantitative comparison with theoretical curves. However, the measured anisotropies formed by taking the differences between profiles measured along various directions will be unaffected by this problem.

The experimental profiles are given in Table 2 at a selection of momentum values. The data were obtained on a grid of 0·05 a.u. by making a linear interpolation between the original data points from the multichannel analyser (which has a non-equidistant channel spacing of about 0·03 a.u. on the momentum scale). This procedure, together with the removal of the asymmetric resolution effects, has reduced some of the statistical fluctuations on the data points. A theoretical profile for Li_3N derived from the Watson-sphere model for N^{3-} and a free-ion Li^+ is also given in Table 2.

5. Discussion

We consider first of all the degree to which the N^{3-} Watson-sphere model represents an improvement over the free-atom $Li_3^0N^0$ configuration in describing the electron distribution in the crystal. Schulz & Schwarz (1978) made a similar comparison when analysing their

Table 2. *Experimental Compton profiles for* Li_3N *measured along three dimensions*

The theoretical profile for Li^+N^{3-} was calculated with a Watson radius for N^{3-} of 1·2 Å, and the curve has been convoluted with the experimental resolution function.

	Experimental Compton profiles			Theory* (Watson model)
p_z	(001)	(100)	(110)	$r_w = 1{\cdot}2$ Å
0·0	6·731 ± 0·020	6·613 ± 0·030	6·571 ± 0·030	6·713
0·1	6·678	6·561	6·509	6·659
0·2	6·506	6·401	6·335	6·495
0·3	6·191	6·139	6·096	6·222
0·4	5·788	5·770	5·782	5·849
0·5	5·318	5·338	5·377	5·396
0·6	4·808	4·878	4·926	4·892
0·7	4·322	4·404	4·454	4·371
0·8	3·854	3·948	3·974	3·861
0·9	3·411	3·513	3·493	3·385
1·0	3·014 ± 0·015	3·077 ± 0·020	3·039 ± 0·020	2·955
1·2	2·299	2·323	2·257	2·250
1·4	1·756	1·727	1·710	1·731
1·6	1·351	1·333	1·332	1·355
1·8	1·054	1·053	1·072	1·079
2·0	0·837 ± 0·008	0·845	0·871	0·872
2·5	0·540	0·555	0·555	0·539
3·0	0·364	0·359	0·363	0·359
3·5	0·249	0·241	0·255	0·249
4·0	0·180 ± 0·003	0·172 ± 0·005	0·181 ± 0·005	0·177
4·5	0·138	0·125	0·131	0·128
5·0	0·102	0·092	0·097	0·096
6·0	0·057	0·057	0·057	0·055
7·0	0·034 ± 0·002	0·034 ± 0·002	0·034 ± 0·002	0·033

* Includes resolution effects.

X-ray diffraction data. By varying the value of the Watson radius, r_W, between 1·0 and 2·0 Å, they found an optimal R value of 0·009 for an r_W of 1·39 Å (for the 233 K data set), whereas the R value for the free-atom form factor was 0·020.

Fig. 3 shows the Compton profiles for the free atom, the Watson-sphere model with $r_W = 1{\cdot}0$, 1·2 and 1·4 Å and the experimental profile for (001) taken from Table 2. The free-atom profiles and the 1s profile for the Li^+ ion are taken from the Hartree–Fock Clementi profiles tabulated by Weiss, Harvey & Phillips (1968). It is clear from Fig. 3 that the ionic model represents a dramatic improvement over the free-atom model in describing the electron structure of Li_3N. This is primarily because of the extremely diffuse nature of the 2s electron in Li^0 which is drastically modified in the solid. It can also be seen that, below about 2·0 a.u., the Compton profile is rather sensitive to the Watson-sphere parameter, r_W. Since Compton-profile errors at the peak are well under 1%, it is possible to specify a very precise optimal r_W. However, an inspection of the experimental profiles in Table 1 reveals a directional variation of more than 2% in the peak height. Therefore, it is sufficient to say that, when using the wave functions calculated by Schwarz & Schulz (1978), a choice of r_W close to 1·2 Å provides a very satisfactory description of the isotropic Compton profile in Li_3N.

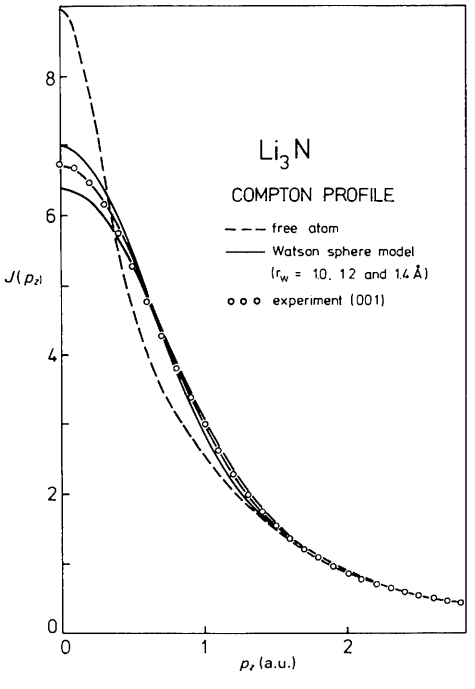

Fig. 3. Experimental and theoretical Compton profiles of Li_3N. In each case the theoretical curves have been convoluted with the experimental resolution function. Theoretical profiles from the Watson-sphere model are indicated by the continuous curves; their peak values are 6·402, 6·713 and 6·990 a.u.$^{-1}$ for Watson-sphere radii of 1·0, 1·2 and 1·4 Å, respectively. Experimental error bars are smaller than the diameter of the circles which indicate the experimental points.

It is interesting to note that the Compton results favour a somewhat lower r_W value for the Watson model than the X-ray diffraction study. Because of the good fit between the experimental Compton profile and the theoretical curve over the whole momentum range, it is difficult to point to a source of systematic error which could have produced an additional flattening of the profile. The effect of multiple scattering, for example, is to transfer momentum from the low-momentum region to a broad range above 1·5 a.u., and hence the very good agreement in the high-momentum region excludes this possibility. On the other hand, the diffraction study makes a convincing case for the larger value of r_W since measurements were performed on different samples and at various temperatures with consistent results. Because of the coupling between temperature factors, extinction correction and scaling factor in the structure refinement, it is difficult to isolate a possible source of error in the diffraction work. However, the evidence for a particular r_W value depends crucially upon only a few, low-order reflections below 0·3 Å^{-1}. These are also amongst the strongest reflections and therefore are those most likely to be influenced by extinction. If the method of extinction correction adopted in the refinement procedure was not able to take account of all extinction effects, then the resulting R factor would favour too large a value of r_W.

It is possible that the small discrepancy between Compton and diffraction measurements stems not from some systematic error in the experiments, but is rather due to the different nature of the physical quantities obtained from the two experiments. In order to illustrate this argument, we can draw on the considerable amount of theoretical work which has already been done on the electron momentum distribution in ionic crystals. In particular, it has been shown that a considerable improvement in the description of the solid state can be achieved by including the effects of wave-function overlap between neighbouring ions by obtaining the orthonormalized crystal orbitals using Löwdin's symmetrical orthogonalization method (see Berggren, Manninen, Paakkari, Aikala & Mansikka, 1977). Although no calculations of this type have been performed for the N^{3-} ion, results are available for the O^{2-} ion in MgO. This should provide a useful guide to the order of magnitude of the overlap effects which can be expected in lithium nitride. Considering only the peak value of the Compton profile, the free-ion configuration Mg^0O^0 yields a value of 7·940 a.u.$^{-1}$ while the wave functions of Yamashita & Asano (1970) obtained from a Watson-sphere model lead to a peak value of 5·931 a.u.$^{-1}$. However, a calculation which included the wave-function overlap in MgO led to a

further reduction in the peak height of the profile to 5·575 a.u.$^{-1}$, *i.e.* a 6% effect (numerical values taken from Table 6.10, Berggren *et al.*, 1977). Similar effects can be seen in the Compton profiles of other, more ideally ionic crystals such as KF, as pointed out by Weyrich (1975). One must then consider whether wave-function overlap could have a larger influence on the Compton profile than on the structure factors. This question has been raised before, and the answer seems to be strongly affirmative. Reed, Eisenberger, Martino & Berggren (1974) made both measurements and calculations of the Compton profile of LiF, and they report an experimental anisotropy of about 2% and a good fit with a tight-binding model. They argue that in those cases where anisotropy results from overlapping charges, the anisotropy of the Compton profile goes linearly with the overlap whereas the form-factor anisotropy goes effectively worse than the square of the overlap. Where the overlap is very small, as in the case of an ionic system (*e.g.* in LiF the overlap terms of the order of 10^{-2}), one can therefore expect that the Compton profile would be more than an order of magnitude more sensitive to the overlap than the elastic-scattering measurement. This argument was placed on a more quantitative basis by Snyder & Weber (1978) who calculated directional Compton profiles for the diatomic molecule F_2. They divided the electron density into atomic (one-centre) and bonding (two-centre) terms. The dominant contribution to the electronic charge density came from the atomic part, containing 17·968 electrons. The overlap charge was only 0·032 electrons, or 0·18% of the total. On the other hand, the contribution of the overlap profile to the total spherical Compton profile at the origin was −0·118, or 2·2% of the total profile. At almost all values of momentum, the relative contribution of the overlap part to the valence atomic part of the Compton profile was an order of magnitude greater than the ratio of the overlap charge to the valence atomic charge. In an even more striking result, the directional Compton profile parallel to the bond had a valence-overlap contribution at the origin of −0·669, or 13·4% of the total Compton profile. Hence, the overlap, two-centre terms give a contribution to the Compton profile along the bond which is almost two orders of magnitude larger than their relative contribution to the total charge density. These theoretical results for F_2 are a clear confirmation of the arguments put forward earlier by Reed, Eisenberger, Martino & Berggren (1974).

If the above arguments concerning the sensitivity of the Compton profile are correct, then one can expect the Compton result to indicate not only a spherical contraction of the wave functions in the crystal, but also the introduction of aspherical terms due to the anisotropic coordination of neighbouring ions. This is indeed the case, and the Compton profile anisotropy is shown in Fig. 4. The way in which the anisotropic behaviour is well reproduced for both positive and negative momenta (corresponding to high- and low-energy sides of the measured energy spectrum), confirms the reliability of the data. It can be seen that the greatest anisotropy can be found by comparing profiles measured with the scattering vector lying in the Li_2N layer and perpendicular to the layer. However, Fig. 4(*b*) also shows that there is significant anisotropy within the Li_2N layer. As an aid to the interpretation of these anisotropy curves, we have Fourier transformed the data in Fig. 4 to obtain the difference curves $\Delta B(z)$ on a position scale shown in Fig. 5. It is immediately clear that the largest effects are occurring in the range between 2·0 and 3·0 Å, although in the case of the difference curve ⟨001⟩ − ⟨110⟩ some anisotropy is already apparent in the range of about 1·0 Å. However, statistically significant differences persist well beyond 3 Å, and it must be remembered that the experimental resolution reduces the amplitude of the longer range information. These results indicate that the anisotropic behaviour in Li_3N is due not only to the nearest-

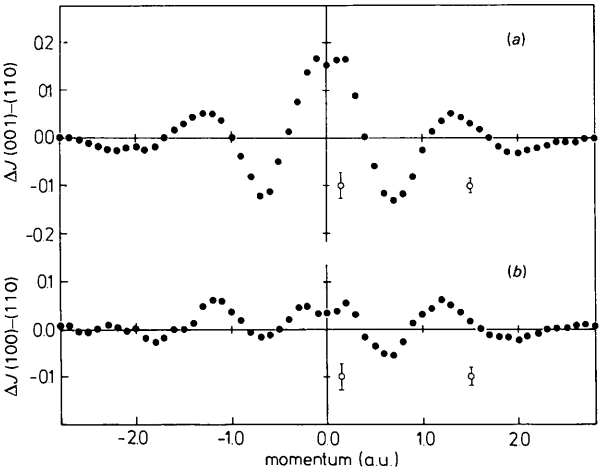

Fig. 4. Experimental Compton-profile anisotropies for Li_3N. The error bars indicate ±1 standard deviation.

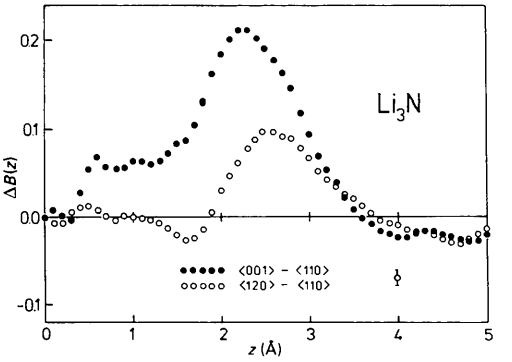

Fig. 5. The Fourier transform of the Compton profile anisotropies shown in Fig. 4. Error bars indicate ±1 standard deviation.

neighbour N–Li interaction but also to the overlap of the more distant, but very diffuse, N ions.

In order to confirm this interpretation of the anisotropy in Li_3N, we can examine the long-range behaviour of each $B(z)$ individually, without having to form any differences. These are shown in Fig. 6 in the range up to 8 Å. (Note the change of scale compared with Fig. 5.) It is apparent from Fig. 6 that something special is happening along the direction ⟨110⟩ which connects neighbouring N ions. This type of sharp negative overshoot in $B(z)$ has already been observed in similar ionic systems such as LiH (Pattison & Weyrich, 1979) and it can definitely be ascribed to the effects of overlap between the diffuse anions. As an additional check on the accuracy and reliability of the experimental data, one can examine the long-range behaviour of $B(z)$ to determine whether the zero passages occur at the correct positions. As pointed out in § 2, the autocorrelation function $B(z)$ in a crystal with filled bands should have a value of zero at all lattice translational vectors, $\mathbf{R}_j$. Those values of $\mathbf{R}_j$ which lie along ⟨001⟩, ⟨120⟩ and ⟨110⟩ are indicated in Fig. 6 by vertical slashes. In all cases the experimental curves pass through zero at the appropriate lattice translational vectors, within the experimental statistics.

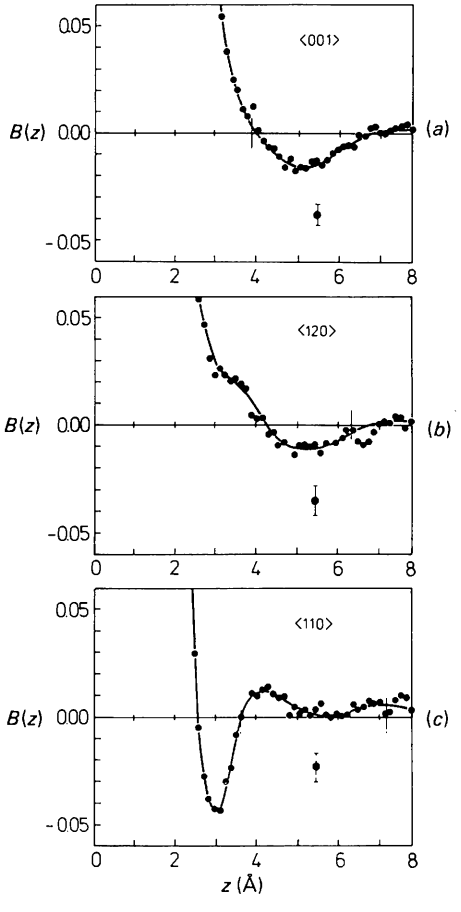

Fig. 6. The autocorrelation function $B(\bar{t})$ along three directions obtained by Fourier transforming the experimental directional Compton profiles. Error bars indicate ±1 standard deviation. The long vertical lines crossing the z axis show the position of translational lattice sites.

6. Concluding remarks

The present Compton-scattering study has confirmed the ionic model of lithium nitride, and provides strong support for the similar conclusions drawn from X-ray diffraction data (Schulz & Schwarz, 1978) and from the dynamic properties of this material (Chandraseka, Bhattacharya, Migoni & Bilz, 1978). However, the sensitivity of the Compton method has allowed us to go beyond the simple Watson model of a free N^{3-} ion. This type of model is unable to describe any anisotropy found in the experimental profiles, although it does appear to provide a reasonable picture of the spherical average. In the absence of any solid-state calculation specifically for lithium nitride, the Fourier transform of the Compton profile has proved to be a useful aid for interpreting the directional properties of the experimental data. However, it is still difficult to distinguish between the influence of neighbouring lithium ions on the nitrogen, and the longer-range effects of overlap between nitrogen ions. It would therefore be useful to see the results of even a relatively crude calculation of the interactions between the diffuse N^{3-} ion and various orders of neighbours.

The small but significant discrepancy between the optimal Watson radius derived from elastic- and inelastic-scattering work represents an interesting challenge to the techniques. Although it is possible that some systematic error could be responsible for this difference, we have argued that this is not necessarily the case. When calculating the momentum density and form factor, even for a spherically symmetric ion, the functional dependence of the two quantities is quite different. This is particularly true for the 2p orbitals, which are the most populous and also the most sensitive to the choice of Watson radius. In addition, we have emphasized the sensitivity of the Compton profile to the effects of wave-function overlap in the crystal, using calculations which are available for MgO to indicate the quantitiative effects which can be anticipated in Li_3N. The way in which two-centre overlap terms can have a far larger effect on the momentum density than on the charge density was also illustrated by using the results of a recent calculation for the F_2 molecule (Snyder & Weber, 1978). For these reasons we suggest that the discrepancy between the optimal parameter in the Watson model deduced from the two techniques may simply be an indication that the

theoretical model is too crude to satisfy both criteria at once.

Since lithium nitride appears to be a useful model substance, the experimental investigation of the electron density will be developed further using both elastic- and inelastic-scattering techniques. A measurement of a few, low-order reflections can be made on an absolute scale using the gamma-ray diffractometer operating at the Hahn-Meitner-Institut. This will provide an independent check on the conclusions drawn from the X-ray diffraction study, which involved the measurement of several hundreds of reflections followed by a standard refinement procedure. Since a change in the Watson-sphere radius, r_W, of 0·2 Å modifies the value of the N^{3-} form factor by about 5%, it should be possible to specify an optimal r_W even using only a few reflections (provided these can be measured on an absolute scale, and corrected for extinction effects). A gamma-ray diffractometer offers just this possibility (Schneider, 1976), whereas the collection of a large data set, suitable for a charge-density refinement, would be very time consuming on such an instrument.

More Compton-profile measurements on this Li_3N crystal are planned for the near future. Attention will be focused on the behaviour of the momentum density in the Li_2N layer. Because of the hexagonal symmetry, it is only necessary to collect data over a range of 30°, and therefore four additional measurements would provide directional Compton profiles on an angular mesh with an interval of only 5°. It would then be possible to make a reliable reconstruction of the projection of the momentum density onto the Li_2N plane, and this should provide a critical test of any theoretical model of the electron density in this material. Since various studies of lithium nitride have indicated that the lithium ions within these layers are responsible for the high lithium mobility (Schulz & Thiemann, 1979), a detailed investigation of this particular projection of the momentum density may throw additional light on the mechanism of ionic conduction in this material.

Thanks are extended to Professor K. Schwarz for providing the numerical wave functions for the nitrogen ion, and to Professor H. Schulz for supplying us with the single crystal of Li_3N (which was prepared at the Max-Planck-Institut für Festkörperforschung in Stuttgart) and for useful discussions concerning the X-ray diffraction measurements. We would also like to thank Dr N. K. Hansen for many helpful suggestions during this work. The financial support of the Deutsche Forschungsgemeinschaft is gratefully acknowledged.

References

BERGGREN, K.-F., MANNINEN, S., PAAKKARI, T., AIKALA, O. & MANSIKKA, K. (1977). In *Compton Scattering*, edited by B. WILLIAMS, pp. 139–208. London: McGraw-Hill.

BONHAM, R. A. & FINK, M. (1974). *High-Energy Electron Scattering*, pp. 21. New York: Van Nostrand Reinhold.

CHANDRASEKA, H. R., BHATTACHARYA, G., MIGONI, R. & BILZ, H. (1978). *Phys. Rev. B*, **17**, 884–893.

COOPER, M., PATTISON, P. & SCHNEIDER, J. R. (1976). *Philos. Mag.* **34**, 243–257.

FELSTEINER, J. & PATTISON, P. (1976). *Phys. Rev. B*, **13**, 2702–2704.

PATTISON, P. & SCHNEIDER, J. R. (1978). *Nucl. Instrum. Methods*, **158**, 145–152.

PATTISON, P. & WEYRICH, W. (1979). *J. Phys. Chem. Solids*, **40**, 213–222.

RABENAU, A. (1978). *Festkörperprobleme*. Vol. XVIII, pp. 77–108. Braunschweig: Vieweg.

REED, W. A., EISENBERGER, P., MARTINO, F. & BERGGREN, K.-F. (1974). *Phys. Rev. Lett.* **35**, 114–117.

SCHNEIDER, J. R. (1974). *J. Appl. Cryst.* **7**, 541–546.

SCHNEIDER, J. R. (1976). *J. Appl. Cryst.* **9**, 394–402.

SCHNEIDER, J. R., PATTISON, P. & GRAF, H. A. (1979). *Nucl. Instrum. Methods*, **166**, 1–19.

SCHÜLKE, W. (1977). *Phys. Status Solidi B*, **82**, 229–235.

SCHULZ, H. & SCHWARZ, K. (1978). *Acta Cryst.* A**34**, 999–1005.

SCHULZ, H. & THIEMANN, K. H. (1979). *Acta Cryst.* A**35**, 309–314.

SCHWARZ, K. (1979). Private communication.

SCHWARZ, K. & SCHULZ, H. (1978). *Acta Cryst.* A**34**, 994–999.

SNYDER, L. C. & WEBER, T. A. (1978). *J. Chem. Phys.* **68**, 2974–2979.

WATSON, R. E. (1958). *Phys. Rev.* **111**, 1108–1110.

WEISS, R. J., HARVEY, A. & PHILLIPS, W. C. (1968). *Philos. Mag.* **17**, 241–253.

WEISS, R. J., REED, W. A. & PATTISON, P. (1977). In *Compton Scattering*, edited by B. WILLIAMS, pp. 43–78. London: McGraw-Hill.

WEYRICH, W. (1975). *Ber. Bunsenges. Phys. Chem.* **79**, 1085–1095.

WEYRICH, W., PATTISON, P. & WILLIAMS, B. (1979). *Chem. Phys.* **41**, 271–284.

WILLIAMS, B. (1977). *Compton Scattering*. London: McGraw-Hill.

YAMASHITA, J. & ASANO, S. (1970). *J. Phys. Soc. Jpn*, **28**, 1143–1147.